On the accuracy of density-functional methods for determining structures of dicationic binuclear ruthenocene derivatives bridged by an unsaturated molecule

Toshiyuki Takayanagi,* Kenta Takahashi, Takashi Fujihara, and Masaru Sato

Department of Chemistry, Saitama University, 255 Shimo-Okubo, Sakura-ku, Saitama City, Saitama 338-8570, Japan

Abstract

Various exchange and correlation functionals have been examined in density-functional calculations for obtaining reliable optimized structures for dicationic binuclear ruthenocenes bridged by an unsaturated compound, which has a characteristic fulvene-type structure. First, we have performed extensive calculations for ruthenocene ($RuCp_2$) in D_{5h} symmetry. It has been found that the Ru-Cp optimized distance is linearly correlated with the energy difference between highest occupied a_1' and e_2' orbitals. We have then found that the optimized structure of dicationic binuclear ruthenocenes is strongly dependent of the a_1'-e_2' orbital sequence observed in $RuCp_2$. In particular, when exchange-correlation functionals giving the $a_1' < e_2'$ orbital sequence are employed, the contribution of the fulvene-type structure is found to be significantly underestimated in the optimized structure of dicationic binuclear ruthenocenes. We finally demonstrate that the SVWN exchange-correlation functions give reasonable optimized structures comparable to experimental structures determined by X-ray crystallography analysis.

---

*To whom correspondence should be addressed: E-mail address: tako@chem.saitama-u.ac.jp

Introduction

Our research group has been interested in synthesis and properties of binuclear ruthenocene derivatives bridged by various unsaturated compounds since it is expected that these molecules can be good candidates for building blocks of molecular wires [1-3]. One of the most important properties of the building block molecule for molecular wires is electron redox behavior; the molecule should be stable in both neutral and oxidized forms. We have previously found that binuclear ruthenocene derivatives bridged by unsaturated organic compounds undergo one-step two-electron redox processes [4-8], which are schematically displayed in Fig. 1. Several unsaturated compounds including oligoenes, oligoynes and thiophenes were employed as a bridging molecule.

The important feature found in the two-electron redox reactions for binuclear ruthenocene derivatives is structural change [4-10], as is also shown in Fig. 1. In two-electron oxidized forms, the fulvene-type structure is generally more stable due to attractive interaction between positively charged ruthenium atoms and C-C double bonds [9,10]. As a result, molecular structures of oxidized species are significantly distorted from those of neutral parent molecules. For example, the C-C bond direction is distorted from the plane of fulvene to allow interaction of the carbon atom with the ruthenium atom (angle β) and two planes of the five-membered rings of ruthenocene is tilted (angle α). In order to understand this structural rearrangement upon oxidization from a theoretical point of view, we have previously performed density-functional calculations at the B3LYP/3-21G level of theory [6,7]. In the case of binuclear ruthenocenes bridged by oligoenes or oligoynes, optimized structures for oxidized species were found to qualitatively agree with structures experimentally determined by X-ray crystal analysis although some deviations were found. However, in the case of thiophenes, we have found that the B3LYP level calculation does not reproduce experimental structures even at qualitative level. In particular, the fulvene-type distortion of the cyclopentadienyl structure was not reproduced in those calculations at all. Instead, we have found that the local spin density approximation (LSDA) level

calculations give relatively good agreement with experimental results [8].

Nowadays, density-functional theory (DFT) is a useful tool in various fields of chemistry since computational costs are comparable to the standard Hartree-Fock calculations. This means that one can easily apply the DFT calculations even to complex organometallic compounds unlike expensive wavefunction-based post Hartree-Fock calculations, by which systematic improvement in accuracy may be possible. However, since the accuracy of the density-functional calculations is generally dependent of exchange or correlation functionals chosen, one should carefully select appropriate exchange and correlation functionals. In this paper, we first apply the DFT calculations using various exchange and correlation functionals to ruthenocene itself in order to evaluate which functional is appropriate for determining structural properties of oxidized binuclear ruthenocene derivatives. Next, we perform the DFT calculations using chosen functionals for oxidized binuclear ruthenocene derivatives and compare optimized structures with the experimental data in great detail. Since accurate prediction of molecular structures is an important first step in electronic structure calculations, we believe that the prescription proposed in this computational study will be useful for future DFT calculations of other complex organometallic molecules.

Computational details

Most of DFT calculations presented in this study were carried out using Gaussian03 package program [11] but some calculations were performed with the Molpro program [12] to confirm converged values in self-consistent field (SCF) calculations. Harmonic vibrational frequency analysis was performed to characterize the optimized geometry as potential minimum on the potential energy surface. All calculations for neutral and dicationic ruthenocene derivatives were performed for singlet spin states and thus spin-restricted Kohn-Sham method was employed. We have also carried out triplet state calculations within the spin-unrestricted Kohn-Sham

method; however, it was found that the singlet state is always more stable than the triplet state in all cases.

As mentioned previously, we have firstly carried out DFT calculations for ruthenocene ($RuCp_2$) with various combination of exchange and correlation functionals. The following standard available pure exchange (E_x) potentials were examined: local spin density approximation (S) [13,14], Becke88 exchange functional (B) [15], Perdew and Wang's 1991 exchange functional (PW91)[16], and Perdew-Burke-Ernzerhof exchange functional (PBE) [17,18]. As for correlation functionals, we have employed the correlation functional of Lee, Yang, and Parr (LYP) [19], Becke's τ-dependent gradient-corrected correlation functional (B95) [20], the gradient corrections of Perdew with his local correlation functional (P86) [21], Perdew and Wang's 1991 gradient-corrected correlation functional (PW91) [16], the gradient-corrected correlation functional of Perdew, Burke and Ernzerhof (PBE) [17,18], the local (non-gradient corrected) functional of Perdew (PL) [22], Vosko, Wilk, and Nusair correlation functional (VWN) [23], and functional V of VWN (VWN5) [23]. We have also used the hybrid version of density-functional methods (B3LYP, B3P86, and B3PW91) [24]. Thus, a total of 35 density-functional methods were examined. Calculations were carried out within D_{5h} symmetry constraint.

For C and H atoms, standard basis sets including 3-21G, 6-31G(*d*), 6-311G, 6-311G(*d*), and 6-311G(*d*, *p*) were employed. On the other hand, we have used both effective core potentials (ECP) and all-electron basis sets for the Ru atom for comparison purpose. The combination of DFT and ECP has been extensively employed in previous theoretical work for molecules containing heavy metal atoms. However, we should notice that the DFT energy is a function of the total electron density. Since some of the total density is excluded from this DFT/ECP combination calculation, it should be emphasized that one has to check carefully the accuracy of this method. Very recently, Alkauskas et al. [25] have studied systematically the accuracy of the DFT/ECP method for small molecules containing Ag and Au. They have demonstrated that the ECPs work well for such molecules. Here, we use a Stuttgart-Dresden-Bonn quasi-relativistic ECP28MWB (SDD) ECP [26] for Ru atoms

in all ruthenocene derivatives. However, for ruthenocene, we have also employed an all-electron double-zeta basis set (DZVP) [27], developed for calculations within local spin density approximation, for comparison purpose.

Results and discussion

Table 1 summarizes optimized distances between Ru and the center of the C_p ring (R(Ru-C_p)) obtained by various combinations of exchange and correlation functionals. It is seen that the optimized distances are in a relatively large range of 1.72-1.92 Å and are strongly dependent of exchange-correlation functionals used. The experimental value is reported to be 1.816 Å from X-ray diffraction analysis [28]. In these geometry optimizing procedures, we have noticed that the symmetry of the HOMO (highest occupied molecular orbital) is either a_1' or e_2', and the corresponding orbital sequence is also dependent of the exchange-correlation functionals employed. In order to understand the correlation between the R(Ru-C_p) distance and orbital sequence, we have plotted the energy difference between the a_1' and e_2' orbitals, $\Delta\varepsilon = \varepsilon(a_1') - \varepsilon(e_2')$, as a function of the R(Ru-C_p) distance as shown in Fig. 2(a). Notice that the positive value of $\Delta\varepsilon$ means that the a_1' orbital is HOMO while the negative value implies that the e_2' orbital is HOMO. A good linear relationship between these two quantities can be clearly seen except for the hybrid density-functional calculations, B3LYP, B3P86 and B3PW91. It should be emphasized that this relationship is essentially the same as the well-known crystal field theory behavior. When attractive interaction between Ru and C_p ring is strong, the optimized R(Ru-C_p) distance becomes shorter and then the a_1' orbital energy level increases. It is interesting to note that the $\Delta\varepsilon = 0$ horizontal line and observed correlation line intersects around R(Ru-C_p) ~ 1.82 Å, which is quite close to the experimental value of 1.816 Å. This suggests that the a_1' and e_2' orbital levels are very close in energy for ruthenocene. Interestingly, it is seen that both the ECP(SDD) and all-electron basis sets give a very similar behavior. This indicates that the core-electron density plays a minor role at least for the orbital

sequence. Also shown in Fig. 2(b) is ionization potential values (no numerical values are presented) as a function of the optimized R(Ru-C_p) distance. If Koopman's theorem was valid, calculated ionization potentials should also correlate to the optimized R(Ru-C_p) distance. However, unlike the a_1'-e_2' orbital energy difference, no clear correlation is seen between these two quantities. It should also be mentioned that the accuracy of the ruthenocene geometry was previously studied using the density-functional method by Swart and Snijders [29]. They have tested various exchange-correlation potentials; however, they did not discuss the geometrical accuracy of neutral ruthenocene in terms of orbital ordering.

From a theoretical point of view, accurate determination of the a_1'-e_2' orbital sequence is somewhat meaningless although the concept of the molecular orbital is quite useful. It is well-known that the concept of the molecular orbital is essentially approximate. In fact, previous experimental studies show that the photoelectron spectrum of ruthenocene in the gas phase is very complicated and that orbital assignment is not easy due to the existence of spin-orbit interaction [30]. However, it should be emphasized that, if the orbital sequence is different, this difference yields different electronic structures for ionized ruthenocenes and then different geometric structures. In order to demonstrate this prediction, we have carried out geometry optimization for binuclear ruthenocene bridged by thiophene using several density-functional methods. Fig. 3 displays molecular geometries of 2,5-bis(ruthenocenyl)thiophene in both neutral and dicationic states optimized using the SVWN (local spin density approximation, LSDA) (a_1' > e_2') and B3LYP density-functional methods (a_1' < e_2') with the 6-311G(d) basis sets. It can be seen that these two methods give very similar optimized structures in neutral states. However, in the case of dicationic state, it is interesting to note that very different optimized structures have been obtained. For the SVWN calculation, the fulvene-type structure is clearly seen and the deformation angle β (see Fig. 1 for definition) was calculated to be 34º. On the other hand, the B3LYP calculation gives β to be only 8º, meaning that thiophene ring and cyclopentadienyl ring are nearly coplanar. The ruthenocene deformation angle α was also found to be different between the SVWN and B3LYP

results (9º vs 15º). The result presented in Fig. 3 thus demonstrates the importance of the a_1'-e_2' orbital sequence [31,32] in electronic structure calculations for cationic ruthenocene derivatives. As shown below, the validity of the SVWN level calculations is supported by comparison to X-ray experimental data [8]. We have also performed BLYP and BPW91 calculations for 2,5-bis(ruthenocenyl)thiophene dication. However, optimized geometries were essentially the same as the B3LYP result though optimized structures are not explicitly presented.

It should be mentioned that the SVWN density-functional calculations were previously performed for ruthenocene by Weber and his co-workers [31,32]. They have discussed the importance of the a_1'-e_2' orbital sequence in excited-state calculations. Interestingly, they have obtained very good agreement between experimental and calculated excited-state properties. Their study also guarantees the accuracy of the SVWN exchange-correlation functionals in ruthenocene and its related compounds.

Since it has been found that the SVWN density-functional calculations give reasonable geometries for dicationic ruthenocene derivatives, we here compare optimized geometries with experimental structures determined by X-ray crystallography analysis [4-8]. In Fig. 4, the computed results are presented for five dicationic molecules including $[RcCCH_3CCH_3Rc]^{2+}$, $[Rc^*C{\equiv}CRc^*]^{2+}$, $[Rc(CH{=}CH)_2Rc]^{2+}$, $[Rc'C{\equiv}CRc']^{2+}$, and $Rc^*C_4H_2SRc^*]^{2+}$ where Rc = ruthenocenyl, Rc* = 1',2',3',4',5'-pentamethylruthenocenyl, and Rc' = 2,3,4,5-tetramethylruthenocenyl. In all cases, agreement between SVWN density-functional results and experimental results is found to be excellent; the differences in bond distances and angles are within ± 0.02 Å and ± 2 degrees, respectively. Fig. 4(b) shows the structure of $[Rc^*C{\equiv}CRc^*]^{2+}$ and the deformation angles, α and β, were calculated to 10.9 and 43.3 degrees, respectively, but previous B3LYP/3-21G calculations [6] gave these values to be 9.2 and 34.5 degrees, respectively. This indicates that the B3LYP/3-21G level calculation somewhat underestimates the contribution of the fulvene-type structure in oxidized species. A similar trend was also seen for $[Rc(CH{=}CH)_2Rc]^{2+}$ (see Fig. 4(c)). Previous B3LYP/3-21G calculations [7] yielded β to be 31.8º and this value is significantly smaller than the SVWN value (38.5°) as well as experimental value (36.2°).

The present study is highly in contrast with a recent DFT computational study by Chizhov and his co-workers [33] for diferrocenyl cumulenes, Fc(Ph)C$_n$(Ph)Fc (n = 2, 4, 6 and 8), which are known to be good molecular objects with great potential in molecular-scale electronics as organic molecular wires. Although they did not examine various combinations of exchange and correlation functionals, they have reported that the B3LYP/6-31G level calculations (the Hay-Wadt pseudopotential was used for Fe) gave good agreement between experimental and calculated properties including structural parameters, electronic transition energies, vibrational frequencies and redox potentials. It should be also mentioned that, in the case of diferrocenyl cumulenes, the spin-multiplicity of the ground electronic state is reported to be triplet for corresponding dicationic molecules. However, as mentioned previously, our calculations showed that the singlet state is always more stable than the triplet state for dicationic binuclear ruthenocene derivatives. This difference is presumably due to the different a_1'-e_2' (a_{1g}-e_{2g} in D_{5d} symmetry) orbital sequence since the symmetry of the HOMO of ferrocene has been previously assigned to be e_{2g} [30]. More systematic calculations would probably be required to understand the difference in spin-multiplicity in various oxidized metallocene derivatives. In addition, calculations of molecular properties other than structural parameters for binuclear ruthenocene derivatives are the next important step and such studied are currently underway in our laboratory.

Concluding Remarks

Electronic structure calculations using DFT are frequently employed to characterize frontier orbitals since these orbitals play essential roles in reactivity as well as properties of molecules. The present computational study strongly suggests that one should carefully select appropriate exchange and correlation functionals to obtain accurate pictures from such electronic structure calculations. At present, we strongly recommend that one should at least employ appropriate functionals that can predict

correct molecular structures since the determination of molecular structures is the important first step of electronic structure calculations. In the case of oxidized binuclear ruthenocene derivatives, we have found that the SVWN (LSDA) exchange and correlation functionals yielded most reliable molecular geometries. This is an unexpected result because the SVWN method is known to be the most primitive one, which does not contain a more sophisticated gradient correction. However, by examining various combinations of exchange and correlation functional in the calculations of ruthenocene in D_{5h} symmetry, we have found that the orbital sequence of highest occupied orbitals play an essential role in determining accurate structural parameters for oxidized binuclear ruthenocene derivatives. This indicates that systematic computational study should be always done in obtaining various electronic properties of complex organometallic molecules. Particularly, special attention should be paid for theoretical prediction of structures of oxidized organometallic molecules. In addition, further improvement in developing more reliable exchange and correlation functions may be necessary from theoretical side in the near future to perform more reliable electronic structure calculations for metallocene derivatives and corresponding charged species.

References

[1] A. Beck, B. Neimer, M. Wieser, Angew. Chem. 105 (1993) 969.

[2] H. Lang, Angew. Chem. 106 (1994) 659.

[3] A. Nakamura, Bull. Chem. Soc. Jpn. 68 (1995) 1515.

[4] M. Sato, Y. Kawata, A. Kudo, A. Iwai, H. Saito, S. Ochiai, J. Chem. Soc. Dalton Trans. (1998) 2215.

[5] M. Sato, M. Watanabe, Chem. Comm. (2002) 1575.

[6] M. Sato, T. Nagata, A. Tanemura, T. Fujihara, S. Kumakura, K. Unomura, Chem. Eur. J. 10(2004) 2166.

[7] M. Sato, Y. Kubota, Y. Kawata, T. Fujihara, K. Unoura, A. Oyama, Chem. Eur. J. 12 (2006) 2282.

[8] Sato *et al*, submitted for publication.

[9] S. Barlow, A. Cowley, J. C. Green, T. J. Brunker, T. Hascall, Organometallics 20 (2001) 5351.

[10] S. Barlow, L. M. Henling, M. W. Day, W. P. Schaefer, J. C. Green, T. Hascall, S. R. Marder, J. Am. Chem. Soc. 124 (2002) 6285.

[11] Gaussian03, Revision B.04, M. J. Frisch et. al, Gaussian, Inc., Pittsburgh PA, 2003.

[12] MOLPRO is a package of ab initio programs written by H.-J. Werner et al.

[13] P. Hohenberg, W. Kohn, Phys. Rev. B 136 (1964) 864.

[14] W. Kohn, L. J. Sham, Phys. Rev. A 140 (1965) 1133.

[15] A. D. Becke, Phys. Rev. A 38 (1988) 3098.

[16] J. P. Perdew, K. Burke, Y. Wang, Phys. Rev. B, 54 (1996) 16533.

[17] J. P. Perdew, K. Burke, M. Ernzerhof, Phys. Rev. Lett. 78 (1997) 1396.

[18] J. P. Perdew, K. Burke, M. Ernzerhof, Phys. Rev. Lett. 77 (1996) 3865.

[19] C. Lee, W. Yang, R. G. Parr, Phys. Rev. B 37 (1988) 785.

[20] A. D. Becke, J. Chem. Phys. 104 (1996) 1040.

[21] J. P. Perdew, Phys. Rev. B 33 (1986) 8822.

[22] J. P. Perdew, A. Zunger, Phys. Rev. B 23 (1981) 5048.

[23] S. H. Vosko, L. Wilk, M. Nusair, Can. J. Phys. 58 (1980) 1200.

[24] A. D. Becke, J. Chem. Phys. 98 (1993) 5648.

[25] A. Bergner, M. Dolg, W. Kuechle, H. Stoll, H. Preuss, Mol. Phys. 80 (1993) 1431.

[26] A. Alkauskas, A. Baratoff, C. Bruder, J. Phys. Chem. A 108 (2004) 6863.

[27] N. Godbout, D. R. Salahub, J. Andzelm, E. Wimmer, Can. J. Chem. 70 (1992) 560.

[28] P. Seiler, J. D. Dunitz, Acta Crystallogr. B 36 (1980) 2946.

[29] M. Swart, J. G. Snijders, Theor. Chem. Acc. 110 (2003) 34.

[30] D. L. Lichtenberger, Y. Elkadi, E. Gruhn, R. P. Hughes, O. J. Curnow, X. Zheng, Organometallics 16 (1997) 5209.

[31] C. Daul, H.-U. Güdel, J. Weber, J. Chem. Phys. 98 (1993) 4023.

[32] F. Gilardori, J. Weber, A. Hauser, C. Daul, J. Chem. Phys. 109 (1998) 1425.

[33] B. Bildstein, O. Loza, Y. Chizhov, Organometallics, 23 (2004) 1825.

Figure Captions

Fig. 1 Schematic representation of two-electron oxidation of binuclear ruthenocenes bridged by an unsaturated molecule. Structural deformation angles, α and β are also defined.

Fig. 2 Energy difference between a_1' and e_2' orbitals, $\Delta\varepsilon = \varepsilon(a_1')-\varepsilon(e_2')$ (a) and ionization potentials (b) as a function of the optimized R(Ru-C_p) distance of ruthenocene. Orbital surfaces are also shown for the a_1' and e_2' orbitals. Solid circles and squares display results calculated with all-electron basis sets for Ru.

Fig. 3 Structural change upon two-electron oxidation for binuclear ruthenocenes bridged by thiophene, $[RcC_4H_2SRc]^{2+}$ (Rc = ruthenocenyl): SVWN (a) and B3LYP (b) results.

Fig. 4 Comparison of SVWN optimized structures of dicationic binuclear ruthenocenes to experimental data (numbers in parentheses) determined by X-ray crystallography analysis: (a) $[RcCCH_3CCH_3Rc]^{2+}$ (b) $[Rc^*C{\equiv}CRc^*]^{2+}$ (c) $[Rc(CH{=}CH)_2Rc]^{2+}$ (d) $[Rc'C{\equiv}CRc']^{2+}$ and (e) $[Rc^*C_4H_2SRc^*]^{2+}$. Disorder[8] has been found for C(17), C(18) and S in $[Rc^*C_4H_2SRc^*]^{2+}$. (Rc = ruthenocenyl, Rc* = 1',2',3',4',5'-pentamethylruthenocenyl, and Rc' = 2,3,4,5-tetramethylruthenocenyl). Distances and angles are in Å and degrees, respectively.

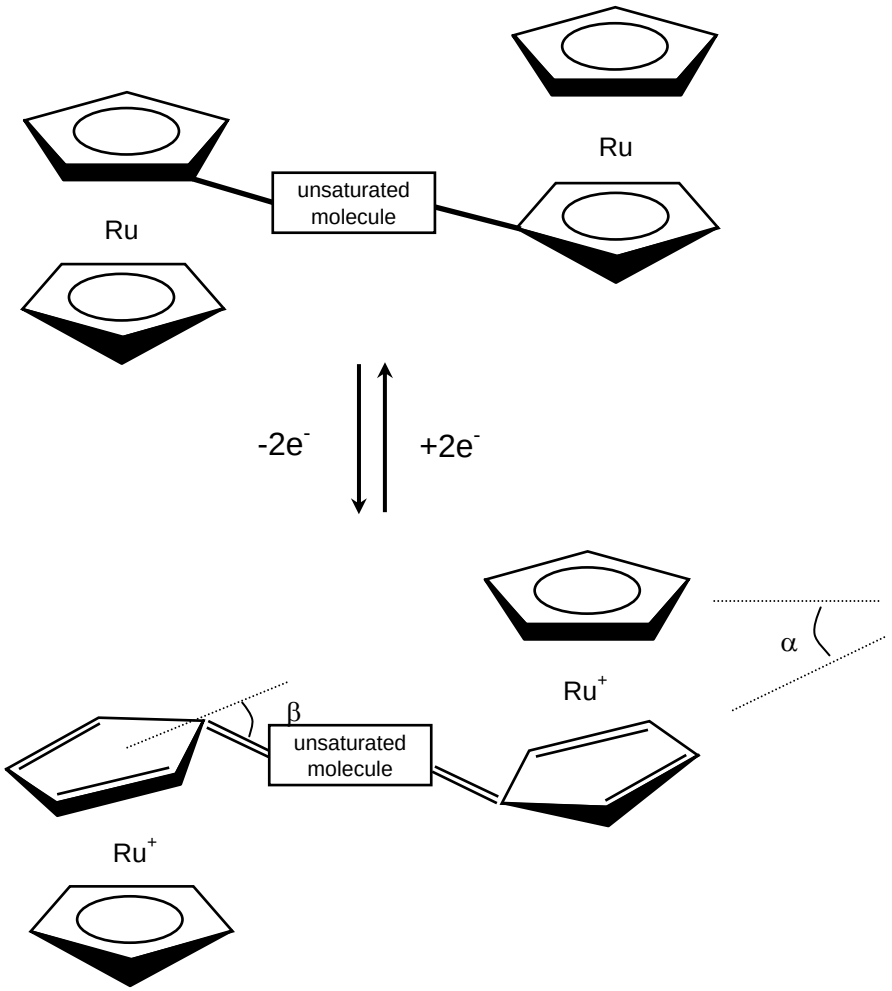
Ru
unsaturated molecule
Ru
-2e-
+2e-
α
Ru+
β
unsaturated molecule
Ru+

Figure 1

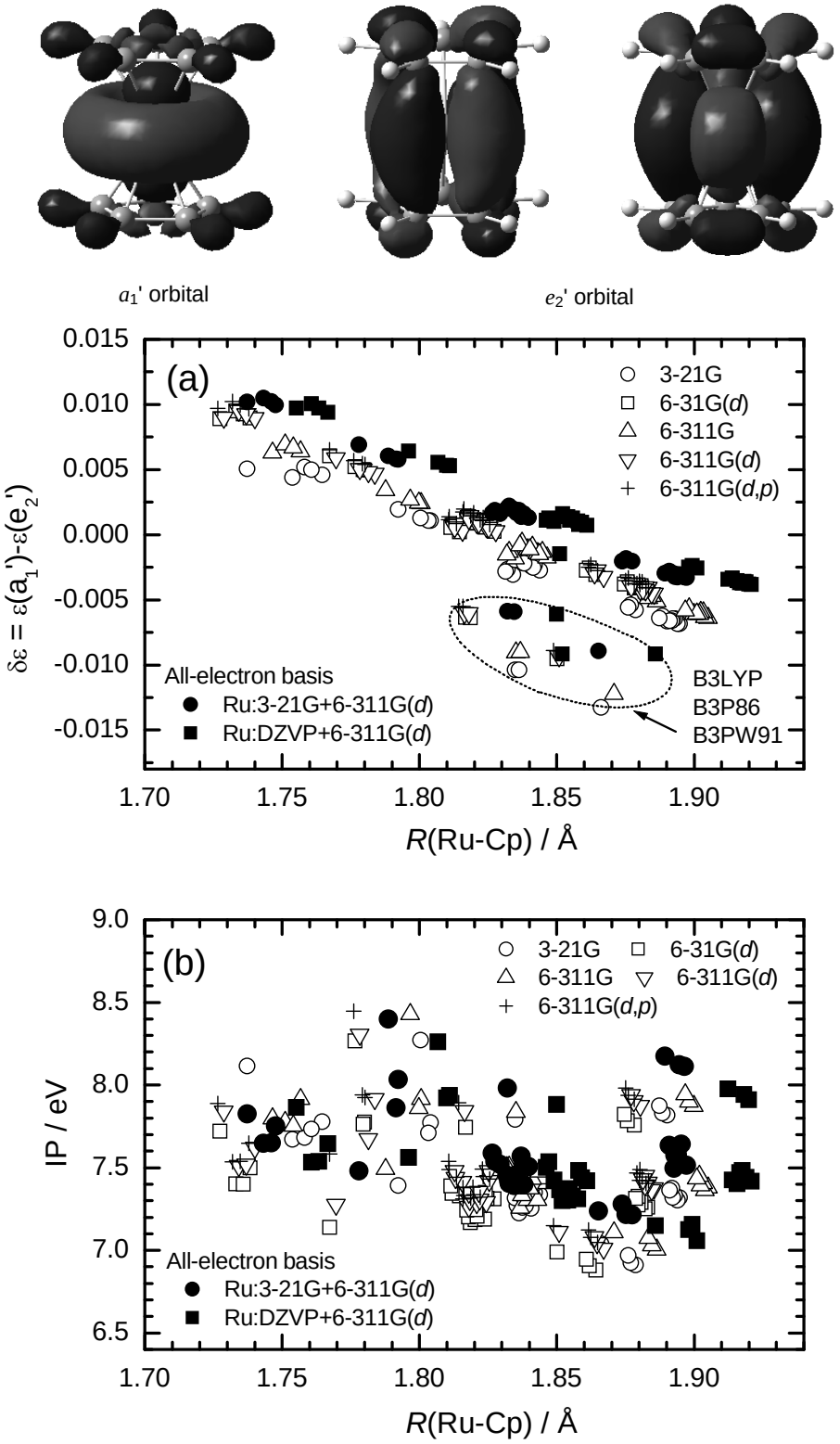
a_1' orbital
e_2' orbital
(a)
3-21G
6-31G(d)
6-311G
6-311G(d)
6-311G(d,p)
All-electron basis
Ru:3-21G+6-311G(d)
Ru:DZVP+6-311G(d)
B3LYP
B3P86
B3PW91
δε = ε(a1')-ε(e2')
R(Ru-Cp) / Å
(b)
IP / eV
R(Ru-Cp) / Å

Figure 2

(a) SVWN

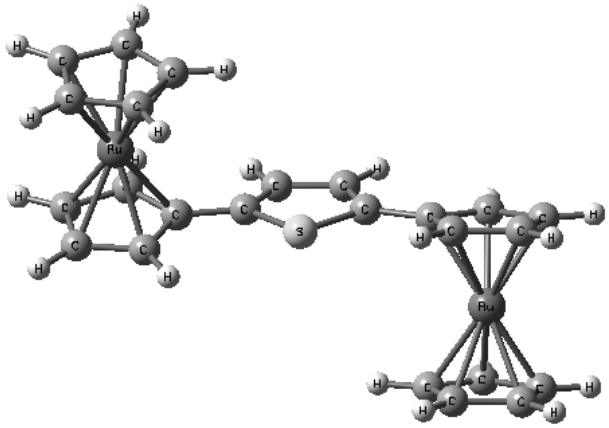

neutral

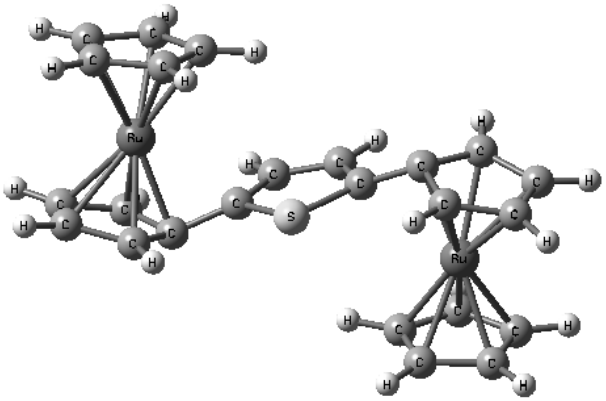

dication

(b) B3LYP

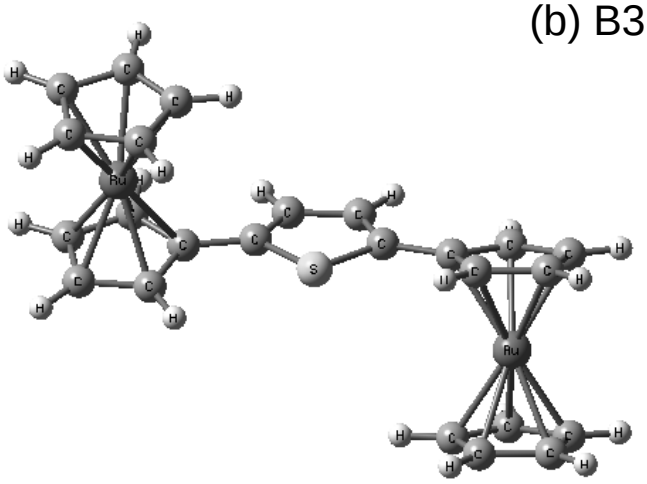

neutral

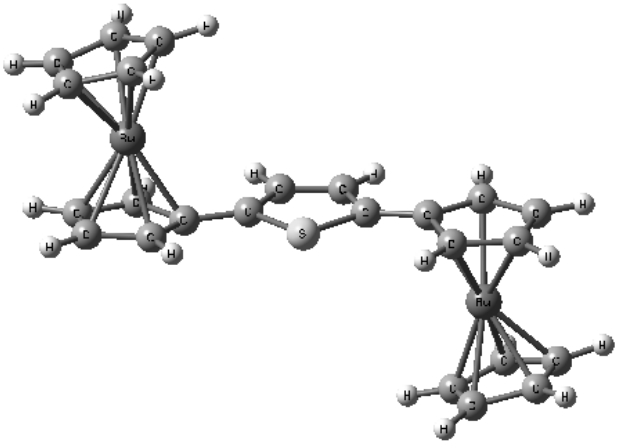

dication

Figure 3

(a) $C_{24}H_{24}Ru_2^{2+}$ (C_2)

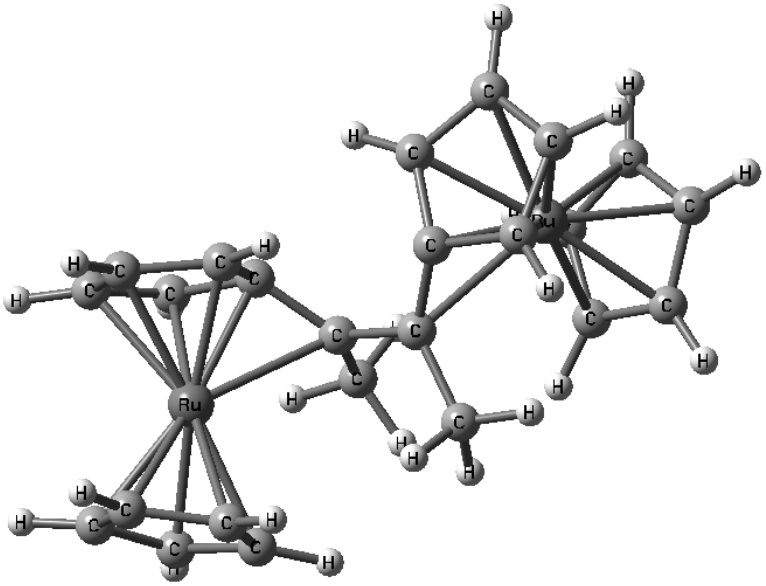

Ru(1)-C(1)	2.443 (2.571)
Ru(1)-C(5)	2.095 (2.116)
Ru(1)-C(6)	2.175 (2.180)
Ru(1)-C(7)	2.229 (2.224)
Ru(1)-C(8)	2.229 (2.217)
Ru(1)-C(9)	2.166 (2.162)
C(1)-C(2)	1.480 (1.491)
C(1)-C(3)	1.491 (1.512)
C(2)-C(4)	1.491 (1.514)
C(1)-C(5)	1.423 (1.406)
C(5)-C(6)	1.460 (1.449)
C(5)-C(9)	1.474 (1.461)
C(6)-C(7)	1.417 (1.395)
C(7)-C(8)	1.436 (1.414)
C(8)-C(9)	1.415 (1.398)
C(2)-C(1)-C(3)	117.9 (117.3)
C(2)-C(1)-C(5)	119.5 (121.1)
C(3)-C(1)-C(5)	120.8 (120.4)
C(1)-C(2)-C(4)	117.9 (116.4)
C(3)-(1)-C(2)-C(4)	60.5 (55.1)
α	11.7 (11.0)
β	35.6 (33.7)

(b) $C_{32}H_{38}Ru_2^{2+}$ (C_i)

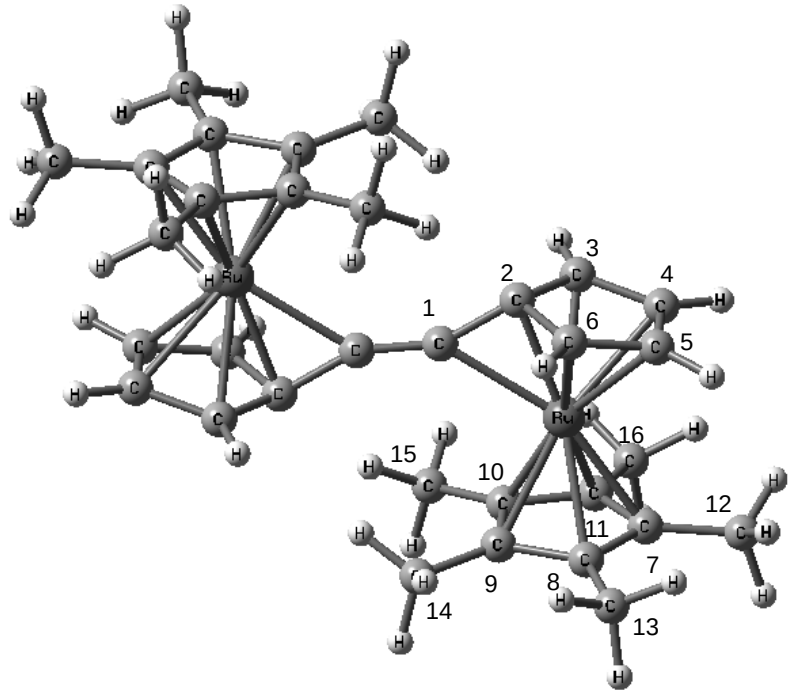

Ru(1)-C(1)	2.231 (2.245)
C(1)-C(1)	1.284 (1.262)
C(1)-C(2)	1.403 (1.405)
C(2)-C(3)	1.471 (1.460)
C(2)-C(6)	1.471 (1.449)
C(3)-C(4)	1.413 (1.401)
C(4)-C(5)	1.439 (1.419)
C(5)-C(6)	1.412 (1.397)
C(1)-C(1)-C(2)	153.8 (153.5)
α	10.9 (11.2)
β	43.3 (41.3)

Figure 4

(c) $C_{24}H_{22}Ru_2^{2+}$ (C_2)

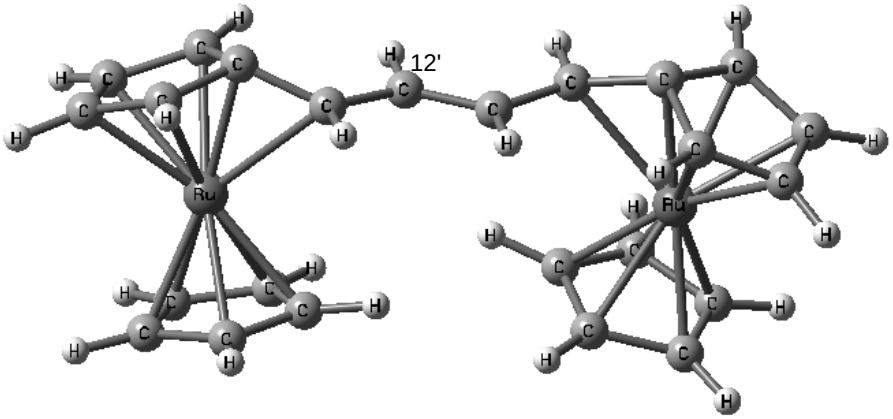

Ru(1)-C(1) 2.083 (2.054) Ru(1)-C(11) 2.356 (2.354)
C(1)-C(11) 1.419 (1.407) C(11)-C(12) 1.433 (1.461)
C(12)-C(12) 1.357 (1.336) C(1)-C(11)-C(12) 124.1 (123.0)
C(11)-C(12)-C(12') 122.8 (122.2) α 8.9 (9.5)
β 38.5 (36.2)

(d) $C_{30}H_{34}Ru_2^{2+}$ (C_i)

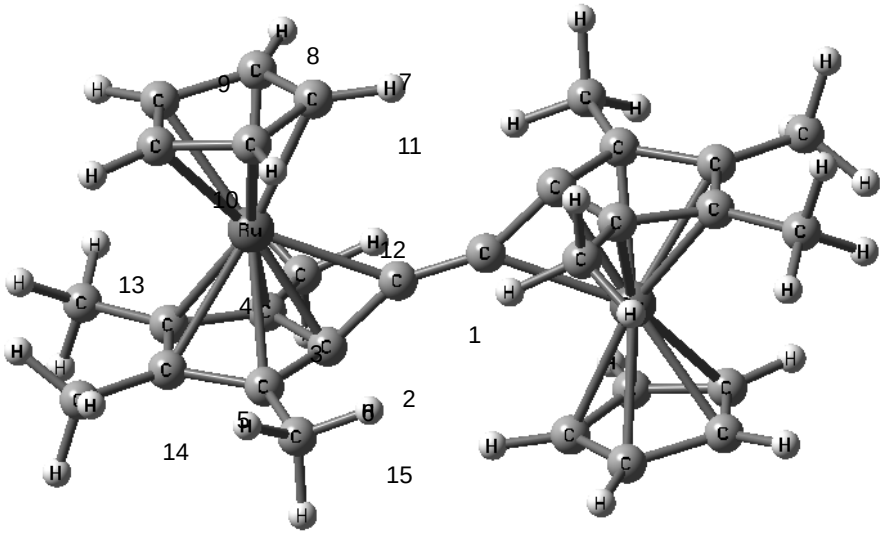

Ru(1)-C(1) 2.169 (2.178)
Ru(1)-C(2) 2.071 (2.067)
Ru(1)-C(3) 2.194 (2.190)
Ru(1)-C(4) 2.259 (2.264)
Ru(1)-C(5) 2.257 (2.261)
Ru(1)-C(6) 2.192 (2.184)
Ru(1)-C(7) 2.194 (2.178)
Ru(1)-C(8) 2.221 (2.192)
Ru(1)-C(9) 2.183 (2.181)
Ru(1)-C(10) 2.182 (2.214)
Ru(1)-C(11) 2.221 (2.179)
C(1)-C(1) 1.290 (1.278)
C(1)-C(2) 1.408 (1.409)
C(2)-C(3) 1.475 (1.467)
C(3)-C(4) 1.427 (1.416)
C(4)-C(5) 1.451 (1.440)
C(5)-C(6) 1.427 (1.412)
C(2)-C(6) 1.475 (1.457)
C(1)-C(1)-C(2) 153.4 (154.1)
C(1)-C(1)-Ru 139.7 (139.5)
C(1)-C(2)-C(3) 115.0 (114.7)
C(1)-C(2)-C(6) 114.8 (115.3)
C(3)-C(2)-C(6) 109.1 (109.7)
C(2)-C(3)-C(4) 105.9 (105.3)
C(3)-C(4)-C(5) 109.5 (109.5)
C(4)-C(5)-C(6) 109.5 (109.8)
C(5)-C(6)-C(2) 105.9 (105.7)
α 10.1 (7.9)
β 45.6 (43.9)

Figure 4

(e) $C_{34}H_{40}SRu_2^{2+}$ (C_2)

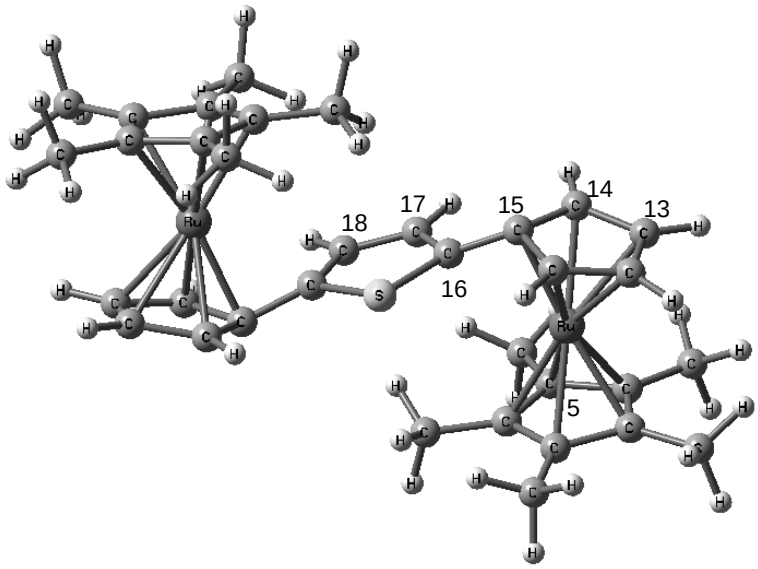

Ru-C(16)	2.499 (2.529)
C(11)-C(12)	1.410 (1.405)
C(11)-C(15)	1.450 (1.439)
C(12)-C(13)	1.430 (1.346)
C(14)-C(15)	1.452 (1.439)
C(15)-C(16)	1.412 (1.381)
C(16)-C(17)	1.431 (1.735)
C(17)-C(18)	1.354 (1.306)
S-C(16)	1.750 (1.560)
S-C(16)-C(15)	122.5.1 (141.8)
S-C(16)-C(17)	109.8 (105.6)
C(16)-C(17)-C(18)	114.1 (110.5)
C(16)-S-C(16)	92.1 (108.2)
α	12.3 (11.9)
β	32.7 (30.5)

Figure 4

Table 1 Optimized distances between Ru and Cp ring (n Å) and energy differences between a_1' and e_2' orbitals (in hartree) for ruthenocene $Ru(Cp)_2$.

		SDD effective core potential for Ru										All-electron basis set for Ru			
Exchange	Correlation	3-21G		6-31G(*d*)		6-311G		6-311G(*d*)		6-311G(*d*, *p*)		6-311G(*d*)+ 3-21G		6-311G(*d*)+ DZVP	
E_x	E_c	R_{Ru-Cp}	Δε	R_{Ru-Cp}	Δε	R_{Ru-Cp}	Δε	R_{Ru-Cp}	Δε	R_{Ru-Cp}	Δε	R_{Ru-Cp}	Δε	R_{Ru-Cp}	Δε
B3	LYP	1.8661	-0.0133	1.8501	-0.0095	1.8708	-0.0122	1.8509	-0.0093	1.8488	-0.0089	1.8652	-0.0089	1.8860	-0.0092
	P86	1.8349	-0.0104	1.8168	-0.0063	1.8351	-0.0091	1.8164	-0.0060	1.8143	-0.0055	1.8321	-0.0059	1.8500	-0.0061
	PW91	1.8363	-0.0104	1.8185	-0.0064	1.8367	-0.0090	1.8180	-0.0060	1.8159	-0.0055	1.8346	-0.0059	1.8520	-0.0092
B	B95	1.8341	-0.0031	1.8145	0.00021	1.8348	-0.0018	1.8156	0.00032	1.8134	0.00085	1.8293	0.0016	1.8490	0.0010
	LYP	1.8787	-0.0058	1.8643	-0.0031	1.8864	-0.0052	1.8670	-0.0032	1.8649	-0.0028	1.8774	-0.0020	1.9011	-0.0026
	P86	1.8438	-0.0027	1.8271	0.00026	1.8465	-0.0018	1.8278	0.00028	1.8256	0.00080	1.8398	0.0013	1.8610	0.00072
	PBE	1.8375	-0.0022	1.8203	0.00088	1.8394	-0.0011	1.8209	0.00092	1.8187	0.0015	1.8346	0.0019	1.8540	0.0014
	PL	1.8947	-0.0068	1.8831	-0.0044	1.9051	-0.0064	1.8855	-0.0045	1.8834	-0.0041	1.8972	-0.0033	1.9209	-0.0038
	PW91	1.8407	-0.0024	1.8237	0.00060	1.8430	-0.0014	1.8244	0.00062	1.8222	0.0012	1.8380	0.0016	1.8577	0.0010
	VWN5	1.8939	-0.0068	1.8822	-0.0043	1.9040	-0.0063	1.8845	-0.0045	1.8824	-0.0040	1.8964	-0.0032	1.9199	-0.0038
	VWN	1.8902	-0.0066	1.8782	-0.0041	1.8999	-0.0061	1.8804	-0.0042	1.8783	-0.0038	1.8927	-0.0030	1.9157	-0.0035
PBE	B95	1.8321	-0.0027	1.8119	0.00073	1.8327	-0.0013	1.8131	0.00085	1.8108	0.0014	1.8274	0.0019	1.8471	0.0013
	LYP	1.8770	-0.0054	1.8619	-0.0026	1.8847	-0.0047	1.8647	-0.0027	1.8624	-0.0023	1.8752	-0.0018	1.8993	-0.0024
	P86	1.8420	-0.0023	1.8247	0.00075	1.8447	-0.0013	1.8254	0.00079	1.8233	0.0013	1.8379	0.0016	1.8591	0.00095
	PBE	1.8355	-0.0018	1.8178	0.0014	1.8374	-0.00064	1.8184	0.0014	1.8162	0.0020	1.8327	0.0022	1.8521	0.0016
	PL	1.8930	-0.0065	1.8807	-0.0039	1.9034	-0.0060	1.8832	-0.0040	1.8811	-0.0036	1.8954	-0.0031	1.9190	-0.0036
	PW91	1.8387	-0.0020	1.8211	0.0011	1.8411	-0.00095	1.8220	0.0011	1.8197	0.0017	1.8362	0.0019	1.8558	0.0013
	VWN5	1.8922	-0.0064	1.8797	-0.0039	1.9024	-0.0059	1.8822	-0.0040	1.8801	-0.0036	1.8945	-0.0031	1.9181	-0.0036
	VWN	1.8885	-0.0062	1.8757	-0.0036	1.8982	-0.0057	1.8781	-0.0037	1.8760	-0.0033	1.8909	-0.0028	1.9139	-0.0033
PW91	B95	1.8314	-0.0028	1.8114	0.00054	1.8319	-0.0015	1.8128	0.00060	1.8106	0.0011	1.8266	0.0017	1.8461	0.0011
	LYP	1.8760	-0.0056	1.8608	-0.0027	1.8834	-0.0049	1.8638	-0.0029	1.8616	-0.0025	1.8739	-0.0020	1.8980	-0.0025
	P86	1.8414	-0.0025	1.8240	0.00058	1.8437	-0.0015	1.8253	0.00054	1.8229	0.0011	1.8371	0.0014	1.8580	0.00080
	PBE	1.8349	-0.0019	1.8173	0.0012	1.8366	-0.00085	1.8181	0.0012	1.8159	0.0018	1.8319	0.0020	1.8511	-0.0015
	PL	1.8919	-0.0066	1.8796	-0.0040	1.9020	-0.0061	1.8823	-0.0042	1.8802	-0.0038	1.8939	-0.0033	1.9176	-0.0037
	PW91	1.8381	-0.0022	1.8206	0.00092	1.8402	-0.0011	1.8216	0.00091	1.8194	0.0014	1.8353	0.0017	1.8547	0.0011
	VWN5	1.8911	-0.0066	1.8787	-0.0040	1.9010	-0.0061	1.8813	-0.0042	1.8792	-0.0038	1.8930	-0.0032	1.9166	-0.0037
	VWN	1.8874	-0.0064	1.8746	-0.0038	1.8968	-0.0059	1.8772	-0.0039	1.8751	-0.0035	1.8894	-0.0030	1.9124	-0.0034
S	B95	1.7537	0.0044	1.7274	0.0089	1.7465	0.0063	1.7288	0.0090	1.7265	0.0097	1.7372	0.0102	1.7552	0.0097
	LYP	1.7922	0.0019	1.7673	0.0061	1.7877	0.0034	1.7696	0.0059	1.7673	0.0065	1.7779	0.0069	1.7961	0.0064
	P86	1.7646	0.0046	1.7384	0.0090	1.7567	0.0064	1.7400	0.0090	1.7378	0.0097	1.7476	0.0100	1.7667	0.0094
	PBE	1.7581	0.0052	1.7332	0.0095	1.7511	0.0069	1.7342	0.0095	1.7319	0.0102	1.7432	0.0105	1.7606	0.0101
	PL	1.8040	0.0011	1.7800	0.0050	1.8006	0.0024	1.7838	0.0047	1.7801	0.0054	1.7922	0.0058	1.8109	0.0053
	PW91	1.7607	0.0050	1.7358	0.0093	1.7540	0.0067	1.7369	0.0093	1.7347	0.0100	1.7460	0.0102	1.7634	0.0097
	VWN5	1.8033	0.0011	1.7795	0.0050	1.7998	0.0024	1.7814	0.0048	1.7792	0.0055	1.7915	0.0058	1.8099	0.0053
	VWN	1.8004	0.0013	1.7765	0.0052	1.7967	0.0027	1.7783	0.0051	1.7761	0.0057	1.7886	0.0060	1.8067	0.0056